Plasmonic Airy beams with dynamically controlled trajectories

Peng Zhang,[1,2,†] Sheng Wang,[1,†] Yongmin Liu,[1,†] Xiaobo Yin,[1,3] Changgui Lu,[1] Zhigang Chen,[2] and Xiang Zhang[1,3,*]

[1]*NSF Nanoscale Science and Engineering Center, 3112 Etcheverry Hall, University of California, Berkeley, California 94720, USA*

[2]*Department of Physics and Astronomy, San Francisco State University, San Francisco, California 94132, USA*

[3]*Materials Science Division, Lawrence Berkeley National Laboratory, 1 Cyclotron Road, Berkeley, California 94720, USA*

**Corresponding author: xiang@berkeley.edu*

Received June 20, 2011; revised July 21, 2011; accepted July 21, 2011;
posted July 22, 2011 (Doc. ID 149581); published August 11, 2011

We report the experimental generation and dynamic trajectory control of plasmonic Airy beams (PABs). The PABs are created by directly coupling free-space Airy beams to surface plasmon polaritons through a grating coupler on a metal surface. We show that the ballistic motion of the PABs can be reconfigured in real time by either a computer addressed spatial light modulator or mechanical means. © 2011 Optical Society of America

OCIS codes: 240.6680, 050.1940.

Surface plasmon polaritons (SPPs) have been studied extensively for many decades due to their abilities to highly enhance optical fields and manipulate light at an extremely small scale beyond the diffraction limit [1]. To manipulate SPPs over a metal surface, which is essential for building ultracompact integrated photonic circuits, different plasmonic elements such as waveguides, lenses, and beam splitters have been proposed [2–4]. However, they all rely on fabricated permanent nanostructures, which are difficult to reconfigure. Recently, nondiffracting Airy beams [5,6] have been theoretically proposed for routing plasmon waves over a metallic interface [7,8]. In comparison with traditional two-dimensional nondiffracting beams [9], such Airy beams represent the only possible nondiffracting wave packets in one-dimensional (1D) planar systems [10]. In addition to the nondiffracting and self-healing properties [11], the propagation of Airy beams exhibits an unique self-bending behavior in the absence of any external potential, which has been exploited for many applications [12–14].

In this Letter, we experimentally demonstrate the generation and dynamic control of plasmonic Airy beams (PABs). By directly coupling 1D Airy beams from free space to SPPs on a metal surface through a grating coupler, we show that the excited PABs can propagate along parabolic trajectories while maintaining the nondiffracting nature. Furthermore, we demonstrate the capability of dynamic routing of SPPs by controlling the ballistic motion of the PABs with either mechanical adjustment of the launch condition or a computer addressed spatial light modulator (SLM). This provides a novel approach to manipulate the flow of SPPs without any waveguide structure over metallic surfaces against surface roughness and defects, even getting over obstacles, which is promising for applications in reconfigurable optical interconnections and on-chip nanoparticle tweezing.

The experimental setup is schematically depicted in Fig. 1. To excite PABs, we first generate a 1D Airy beam in free space ($\lambda = 820$ nm) with a cubic phase mask provided by a computer addressed SLM and Fourier transformation through an objective lens O_1 (20X; NA = 0.75) [6,11]. Then it is directly impinged onto a grating with a period of 805 nm, line width of 400 nm, and height of 80 nm fabricated by electron beam lithography on the top of a 50 nm thick gold film resting on a quartz substrate (see Fig. 1). The polarization of the beam is adjusted to be perpendicular to the grating through a half-wave plate. The excited PAB is directly monitored via leakage radiation microscopy [4] with an oil immersion objective lens O_2 (40X; NA = 1.3) and a CCD camera. In order to dynamically modulate the path of the PABs, as depicted in the inset of Fig. 1, we introduce either mechanical transverse (δ_{ox}) [15] and longitudinal (δ_{oz}) displacements of the objective lens O_1 or computer controlled displacements of the transverse positions of the input Gaussian beam (δ_g) and the cubic mask (δ_m) with respect to the optical axis of O_1 [16].

Following similar theoretical treatments to those described in [5,15,16] and taking the paraxial approximation, an excited PAB can be determined (assuming the position of the grating coupler is at $y = 0$) by

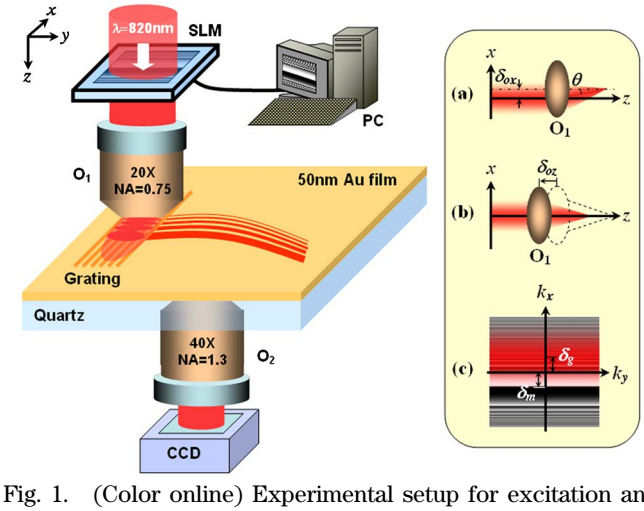

Fig. 1. (Color online) Experimental setup for excitation and observation of PABs. SLM, spatial light modulator; O, objective lens; CCD, charge-coupled device; PC, computer. Inset, (a) and (b) depict the mechanical displacements of O_1 along the transverse x axis (δ_{ox}, resulting a tilt angle θ) and the longitudinal z axis (δ_{oz}); (c) illustrates the computer controlled displacements of the cubic phase mask δ_m and input Gaussian beam δ_g in the SLM with respect to the optical axis of O_1.

$$\phi(x,y) = C \cdot F \cdot G \cdot Q \cdot \mathrm{Ai}[x - (v+\delta_m)(y-\delta_{oz}) - (y-\delta_{oz})^2/4 + i\alpha(y-\delta_{oz}-2\delta_g+2\delta_m)], \quad (1)$$

where $C = \exp[-\alpha(\delta_g-\delta_m)^2 + i2\alpha^2(\delta_m-\delta_g)]$, $F = \exp[\alpha x + \alpha(y-\delta_{oz})(\delta_g - 2\delta_m - v) - \alpha(y-\delta_{oz})^2/2]$, $G = \exp\{i[(v+\delta_m)(x - y^2/2 + y\delta_{oz} - \delta_{oz}^2/2) + (x - v^2 - \delta_m^2 + \alpha^2)(y-\delta_{oz})/2 - (y-\delta_{oz})^3/12]\}$, $Q = \exp(-\beta y)\cdot\exp(-ix^2/d)$, Ai denotes the Airy function, the coordinates x and y are respectively normalized by an arbitrary transverse scale x_0 and kx_0^2, k is the wave vector of SPPs at a wavelength of 820 nm, α is the exponential truncation factor, β is the decay constant due to the loss of the system, and $d = 2f^2/[kx_0^2(l-f)]$ determines the quadratic phase factor due to the Fourier transform process with O_1, f is the focal length of O_1, l is the distance between the cubic phase mask and O_1, and $v = k\theta x_0$ is associated with the tilt angle θ due to δ_{ox}. Without taking into account of the loss and quadratic phase factor, i.e., $Q = 1$, we can readily obtain the trajectory of the PABs as

$$x = (v+\delta_m)(y-\delta_{oz}) + (y-\delta_{oz})^2/4, \quad (2)$$

with the peak intensity occurring at $y = \delta_{oz} + 2(\delta_g - \delta_m)$.

Equation (2) indicates that, similar to the free-space cases, without any modulation, a truncated PAB undergoes parabolic motion with peak intensity at the beginning of the beam path [5–7]. The tilt of the input free-space Airy beam v introduced by the transverse displacement of O_1 (δ_{ox}) only influences the trajectory of the Airy beam, while its peak intensity position is unchanged [15]. However, the longitudinal displacement of O_1 (δ_{oz}) can modulate the beam path while setting the peak intensity position always at the maximum height of the trajectory. In addition, by manipulating the displacements of the input Gaussian beam δ_g and the cubic phase mask δ_m with the computer addressed SLM, we can set not only the PAB into a general ballistic motion but also its peak intensity to different positions along the curved beam path [16]. However, due to the existence of the loss and quadratic phase factor ($|Q| \neq 1$), such PAB control is modified. Specifically, the loss of the system and the quadratic phase factor at $d < 0$ always bring the peak intensity position toward the launch grating. However, when $d > 0$, the phase factor tends to set the peak intensity position close to the apex of the trajectory.

To perform experimental demonstrations, we start from the excitation of PABs without any additional modulation. Figure 2(a) shows the intensity pattern of a typical free-space Airy beam after the SLM and O_1. A SEM image of the grating coupler is shown in Fig. 2(b). Figures 2(c)–2(f) depict our experimental results as well as the corresponding numerical simulations based on Eq. (1). As expected, the PAB indeed propagates along a parabolic path with its peak intensity at the very beginning [see Figs. 2(c) and 2(e)]. By rotating the half-wave plate by 90°, the observed PAB vanishes, indicating the SPP nature of the beam. In comparison, a Gaussian plasmonic beam with a size (3 μm diameter at beam waist) and intensity similar to the main lobe of the PAB shown in Fig. 2(c) propagates along a straight line while suffering apparent divergence and decay [see Figs. 2(d) and 2(f)]. Although the observed Airy beam also experiences diffraction and decay during propagation due to the truncation and loss, it maintains its size and intensity much better than the Gaussian beam does, reflecting the nondiffracting nature of the Airy beam. Our experimental results agree well with the numerical simulations.

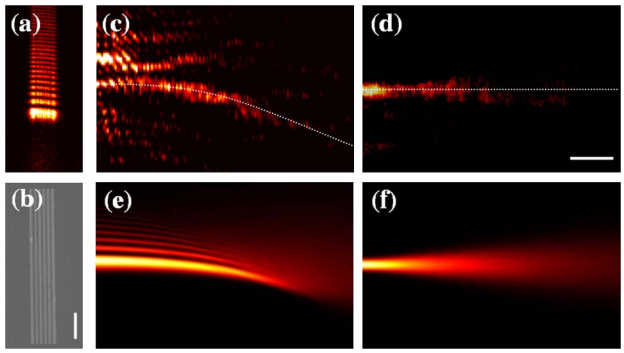

Fig. 2. (Color online) (a) Typical free-space Airy beam projected onto the grating, (b) the SEM image of the grating coupler, (c), (d) leakage radiation microcopy results showing the propagations of a PAB and a Gaussian beam launched from the grating, respectively, (e), (f) the numerical simulation results corresponding to (c) and (d). The dashed lines in (c) and (d) serve for eye guidance. The scale bar shows 5 μm.

For dynamic control of the PAB, we first introduce a tilt angle θ to the input free-space Airy beam at the grating coupler as illustrated in inset (a) of Fig. 1, while keeping the other conditions unchanged. By continuously moving O_1 along the x direction with respect to the optical axis of the system, the tilt angle can be gradually changed, resulting in a real-time change in the beam trajectory without any retardation. Two typical experimental results at $\theta = 7°$ and 28° are displayed in Figs. 3(a) and 3(b), respectively. Apparently, the trajectory of the PAB is switched into a general ballistic one by the tilted excitation, while the peak intensity is always kept at the beginning of the trajectory. Such tilted-excitation-induced control agrees with our theoretical analyses from Eq. (1), confirmed by the numerical simulations as shown in Figs. 3(c) and 3(d).

Similarly, by introducing a displacement to the Fourier lens O_1 along the longitudinal z direction as illustrated in inset (b) of Fig. 1, we can modify the ballistic motion of the generated PAB. Specifically, when O_1 moves closer to the grating coupler, the trajectories will be switched into general projectiles with different maximum heights and ranges. Figure 4(a) displays a typical experimental result, with the corresponding simulation shown in Fig. 4(b). Apparently, the beam propagation range is enlarged along the horizontal direction in comparison with the PAB shown in Figs. 2 and 3. In addition, the peak intensity always occurs before the theoretically predicated position, i.e., the apex of the trajectory. Such deviations result from the loss and the quadratic phase factor determined by Q.

Finally, we demonstrate the computer controlled routing of SPPs by offsetting of the cubic phase mask and the input beam inside the SLM [see inset (c) of Fig. 1], which offers us an alternative method to perform dynamic control without any mechanical movement of lenses. To control the displacement of the phase mask and the input

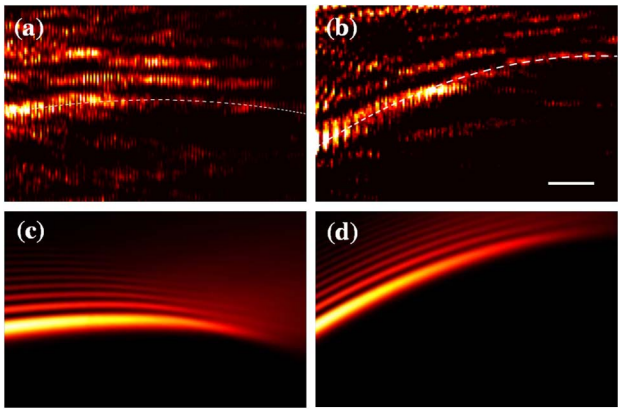

Fig. 3. (Color online) (a), (b) Experimental and (c), (d) numerical results of the generated PABs excited under different incident angles at $\theta = 7°$ [(a), (c)] and $\theta = 28°$ [(b), (d)]. The scale bar shows $5\,\mu$m.

beam, we display an animation of the shifting mask pattern as well as a shifting slit aperture in the SLM. The direction and the speed of the displacement can be controlled at ease. Note that, unlike the approach used in [16], here we use a wide beam illumination onto the SLM, with a computer generated aperture overlaid onto the phase mask. Thus we equivalently modify the beam position. It provides the full control of the Airy beam with computer addressed SLM. In our experiment, as expected from the theory, simply by moving the phase mask, the trajectory is turned into a general ballistic one. By manipulating the beam position, we can indeed move the peak intensity toward the descending side of the parabolic curve. However, in our current experimental setting, such control is challenging, due to the nontrivial quadratic phase factor and the loss. Figures 4(c) and 4(d) show one example of our computer based control, from which we can see that the trajectory of the PAB exhibits a typical ballistic trajectory, and the peak intensity is set at the maximum height of the trajectory. With such a trajectory, it can be expected that SPPs should be able to be redirected at a target along a curved path, surpassing certain obstacles as illustrated in Figs. 4(c) and 4(d).

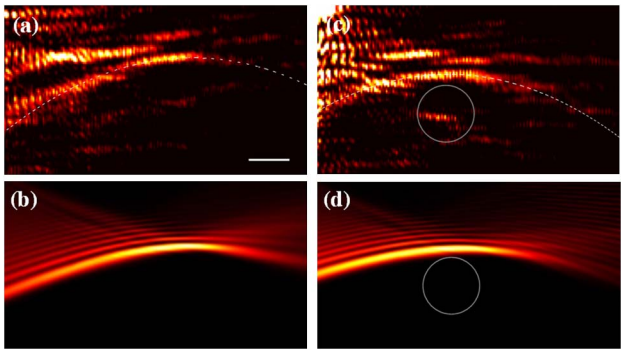

Fig. 4. (Color online) (a), (c) Experimental and (b), (d) numerical results of the PABs generated in the presence of a $25\,\mu$m longitudinal displacement of the objective lens O_1 toward the grating coupler [(a), (b)] and transverse displacements of the cubic phase mask (−3 mm) and the input Gaussian beam (1 mm) in the SLM [(c), (d)]. The added gray solid circles in (c) and (d) mimic obstacles. The scale bar shows $5\,\mu$m.

In summary, we have generated PABs and demonstrated the capability of dynamic control of their ballistic trajectories. Along with the inherent self-healing property of nondiffracting beams, we expect our results could be directly applied for on-chip directional routing of SPP energy along arbitrary trajectories [17] and dynamic manipulations of nanoparticles on metal surfaces [18]. Moreover, our method may be directly employed to excite other types of nondiffracting surface waves, such as surface phonon polaritons and acoustic surface waves.

Note: In finishing this Letter, we noticed an independent work from another group on a similar topic but based on a different method [19].

This work was supported by the United States Army Research Office (USARO) MURI program (W911NF-09-1-0539), the United States Air Force Office of Scientific Research (USAFOSR) (FA9550-09-1-0474), the National Science Foundation (NSF) Nanoscale Science and Engineering Center (CMMI-0751621), and the NSF (PHY-0800972). We thank T. Zentgraf, Y. Park, B. Kante, Z. Ye, and Y. Hu for assistance and discussion.

†These authors contributed equally to this work.

References

1. W. L. Barnes, A. Dereux, and T. W. Ebbesen, Nature **424**, 824 (2003).
2. V. S. Volkov, E. Devaux, J.-Y. Laluet, T. W. Ebbesen, and S. I. Bozhevolnyi, Nature **440**, 508 (2006).
3. E. Devaux, J.-Y. Laluet, B. Stein, C. Genet, T. Ebbesen, J. -C. Weeber, and A. Dereux, Opt. Express **18**, 20610 (2010).
4. T. Zentgraf, Y. Liu, M. H. Mikkelsen, J. Valentine, and X. Zhang, Nat. Nanotechnol. **6**, 151 (2011).
5. G. A. Siviloglou and D. N. Christodoulides, Opt. Lett. **32**, 979 (2007).
6. G. A. Siviloglou, J. Broky, A. Dogariu, and D. N. Christodoulides, Phys. Rev. Lett. **99**, 213901 (2007).
7. A. Salandrino and D. N. Christodoulides, Opt. Lett. **35**, 2082 (2010).
8. W. Liu, D. N. Neshev, I. V. Shadrivov, A. E. Miroshnichenko, and Y. S. Kivshar, Opt. Lett. **36**, 1164 (2011).
9. J. Durnin, J. J. Miceli Jr., and J. H. Eberly, Phys. Rev. Lett. **58**, 1499 (1987).
10. M. V. Berry and N. L. Balazs, Am. J. Phys. **47**, 264 (1979).
11. J. Broky, G. A. Siviloglou, A. Dogariu, and D. N. Christodoulides, Opt. Express **16**, 12880 (2008).
12. J. Baumgartl, M. Mazilu, and K. Dholakia, Nat. Photon. **2**, 675 (2008).
13. P. Polynkin, M. Kolesik, J. V. Moloney, G. A. Siviloglou, and D. N. Christodoulides, Science **324**, 229 (2009).
14. A. Chong, W. Renninger, D. N. Christodoulides, and F. W. Wise, Nat. Photon. **4**, 103 (2010).
15. G. A. Siviloglou, J. Broky, A. Dogariu, and D. N. Christodoulides, Opt. Lett. **33**, 207 (2008).
16. Y. Hu, P. Zhang, C. Lou, S. Huang, J. Xu, and Z. Chen, Opt. Lett. **35**, 2260 (2010).
17. E. Greenfield, M. Segev, W. Walasik, and O. Raz, Phys. Rev. Lett. **106**, 213902 (2011).
18. M. Righini, A. S. Zelenina, C. Girard, and R. Quidant, Nat. Phys. **3**, 477 (2007).
19. A. Minovich, A. E. Klein, N. Janunts, T. Pertsch, D. N. Neshev, and Y. S. Kivshar, in *Quantum Electronics and Laser Science Conference*, OSA Technical Digest (CD) (Optical Society of America (2011), paper QThQ6.